

# Speeding up HMRF\_EM algorithms for fast unsupervised image segmentation by Bootstrap resampling: Application to the brain tissue segmentation

S. M'hiri, L. Cammoun\*, F. Ghorbel

*GRIFT Research Group, CRISTAL Laboratory, National School of Computer Sciences, University of Manouba, Tunisia*

Received 28 May 2006; received in revised form 9 April 2007; accepted 11 April 2007

Available online 25 April 2007

## Abstract

This work deals with global statistical unsupervised segmentation algorithms. In the context of Magnetic Resonance Image (MRI), an accurate and robust segmentation can be achieved by combining both the Hidden Markov Random Field (HMRF) model and the Expectation-Maximization (EM) algorithm. This EM–HMRF approach is accomplished by taking into account spatial information to improve the segmentation process which, in turn, slows the approach and consequently prevents its adoption for real-time applications such as three-dimensional medical image segmentation.

We propose in this paper the use of the Bootstrap resampling to speed up the processing time of the EM–HMRF algorithm. This is accomplished by randomly selecting an optimal representative set of pixels according to some criteria originally defined for the blind segmentation. We will show how to adapt such criteria to the HMRF\_EM algorithm context. We validated our proposition through a set of experiments and we proved that the use of the Bootstrap resampling yields the same accuracy and robustness as the basic algorithm, yet it amounts to a considerable processing speed up.

© 2007 Elsevier B.V. All rights reserved.

**Keywords:** Parameters estimation; Classification; Cerebral brain segmentation; Expectation Maximization; Bootstrap; Sampling; Resampling; EM; Markov Random Field; HMRF\_EM

## 1. Introduction

There are numerous ways to perform image segmentation and it is well known that statistical approaches are among the most robust methods in

terms of homogeneous or textured areas. The robustness comes mainly from the manner in which these approaches take into account the ‘noise’ of an image, for example, the noise from acquisition sensors but also the natural variation in light reflectance of imaged objects.

Statistical approaches can be subdivided into three categories, depending on the way the neighborhood influences the classification of a given pixel:

- Local or blind approaches consider that pixels are spatially independent [1].

\*Corresponding author. EPFL STI ITS, Station 11, 1015 Lausanne, Switzerland. Tel.: +41 21 693 46 22; fax: +41 21 693 76 00.

*E-mail addresses:* [Slim.Mhiri@ensi.rnu.tn](mailto:Slim.Mhiri@ensi.rnu.tn) (S. M'hiri), [Leila.Cammoun@epfl.ch](mailto:Leila.Cammoun@epfl.ch) (L. Cammoun), [Faouzi.Ghorbel@ensi.rnu.tn](mailto:Faouzi.Ghorbel@ensi.rnu.tn) (F. Ghorbel).

- Contextual [2] or adaptive [1] methods take into account a neighborhood of limited extent, e.g. a square window around the pixel of interest.
- Global approaches assume that all pixels in an image influence the classification of the pixel of interest [3].

Global approaches are intractable; nevertheless, Markov Random Field (MRF) models offer them a tractable solution. They allow to express the global dependence by using only contextual relationships between neighboring pixels, thanks to the Hammersley–Clifford theorem [4]. These models, and other Markovian ones with tree or chain topologies [5], have been successfully tested and illustrated in a number of areas such as computer vision, pattern recognition and image processing applications [6,7], including image restoration and segmentation, stereo motion analysis, motion recognition, texture analysis, etc.

Before applying some standard Bayesian restoration methods like Maximum A Posteriori (MAP), model parameters have to be estimated in an unsupervised context (Hidden MRF). Several optimization algorithms have been proposed in the last years and the most widely used is the (Expectation-Maximization) EM algorithm which maximizes the likelihood of data (ML criterion). Nevertheless, these methods appear to be difficult to implement in the context of HMRF [8] and some alternative methods have been proposed. In particular, the time-consuming Monte Carlo simulations or the Stochastic Gradient method [9] aim to approach the maximum of the likelihood (ML) in a stochastic manner to remedy the difficulties encountered by the EM method. Several approximations to the ML criterion have been proposed such as the mean field and mode field approaches [10] and extensions [11], or the maximization of the pseudo-likelihood which is, in particular, at the origin of the Iterated Conditional Mode (ICM) [4] and Gibbsian EM [7] algorithms. The Gibbsian EM is an iterative stochastic algorithm which is known to be computationally costly but efficient. In [12], the authors show that an accurate segmentation can be achieved by combining the HMRF model and the EM method into mathematically sound HMRF\_EM framework. This method integrates iteratively the parameter estimation step with the restoration one as done in the mode field algorithm [11].

Even with the significant efforts done to reduce complexity, the computation time is still a limitation

factor for the applicability of HMRF models, despite their efficiency, especially for applications involving large-size images or requiring a high number of thematic classes. In this work, we propose to introduce a Bootstrap resampling scheme [13] in the HMRF\_EM framework to reduce the processing time.

In [14,15], the authors proposed to speed up some segmentation methods based on the blind approach by introducing a Bootstrap resampling technique. Our main goal is to extend this same technique to the global approach where the Bootstrap resampling is performed within the HMRF\_EM framework.

The improvement or speeding up of the segmentation based on the HMRF\_EM method combined with Bootstrap resampling is portrayed on the brain tissue segmentation, where the MRF model is widely employed. Even if the classification methods comparison for brain tissue segmentation is not one of the objective of this work, it is proved in [16] that the HMRF\_EM is one of the most efficient methods for such an application. To validate the Bootstrap efficiency in the HMRF\_EM framework, we have used some synthetic brain images providing a quantitative comparison [17] and often used for tissue classification validation [16,18].

The remainder of this paper is organized as follows. In the next section, a brief description of Bootstrap resampling is introduced within the context of image processing. Section 3 starts with a short description of the HMRF\_EM method and then provides the integration of the Bootstrap resampling. Section 4 discusses the optimal size of the Bootstrap sample in the context of a global segmentation. The comparison of the HMRF\_EM algorithms with and without Bootstrap resampling within the context of brain Magnetic Resonance Image (MRI) segmentation is then presented in Section 5. Finally, some conclusions and future work directions are provided in Section 6.

## 2. The Bootstrap resampling

In 1979, Efron introduced the Bootstrap term to describe the set of random resampling procedures of the observed data to be approached by simulating the statistics of the underlying distribution [13,19]. The Bootstrap theory is based on the convergence of the empirical law of the sample toward the underlying unknown law when the sample size is sufficiently large.

Given a sample of  $N$  independent identically distributed random vectors  $\{X_1, X_2, \dots, X_N\}$  and a real-valued estimator  $\theta(X_1, X_2, \dots, X_N)$  (denoted by  $\hat{\theta}$ ) of the parameter distribution  $\theta$ , to assess the accuracy of  $\hat{\theta}$  the Bootstrap procedure is defined in terms of the empirical distribution function (*edf*)  $F_N$ . This *edf* assigns a probability mass to each observed value of random vectors  $X_i$  for  $i = 1, \dots, N$ .

The *edf* is the maximum likelihood estimator of the observations distribution when no assumption is made. The Bootstrap distribution for  $\hat{\theta} - \theta$  is the one obtained by generating  $\hat{\theta}$  values by sampling independently with replacement from the empirical distribution  $F_N$ . The Bootstrap estimate of the standard error of  $\hat{\theta}$  is the standard error of the Bootstrap distribution for  $\hat{\theta} - \theta$  [20].

In practice, this technique usually requires the generation of a Bootstrap sample (independent drawing with replacement from the empirical distribution). From the Bootstrap sampling a Monte Carlo approximation of the Bootstrap estimate is therefore obtained. The original Bootstrap procedure can be sum up as follows:

- Generate a sample of size  $N$  with replacement from the empirical distribution (Bootstrap sample).
- Compute the value of  $\hat{\theta}$  obtained by using the Bootstrap sample instead of the original sample, which is denoted by  $\theta^*$ .
- Repeat these two steps  $B$  times to obtain a Monte Carlo approximation of  $\theta^*$  distribution.<sup>1</sup>

The key idea of the Bootstrap is that for  $N$  sufficiently large, we expect that both distributions  $\theta^* - \hat{\theta}$  and  $\hat{\theta} - \theta$  are nearly the same. In other words, the variability of  $\theta^*$  (based on  $F_N$ ) around  $\hat{\theta}$  will be similar to the variability of  $\hat{\theta}$  (based on the true population distribution  $F$ ) around its standard deviation for large sample size. In fact, when  $N$  gets larger  $F_N$  comes closer to  $F$ , and sampling with replacement from  $F_N$  is almost like random sampling from  $F$ .

Classically, the Bootstrap method is used only when the distribution cannot be estimated analytically. However, it is interesting to see that the Bootstrap resampling is also valid in situations where sample size is enough to handle the estimation

[20,21]. Efron gives a set of examples about that, and establishes the validity of the approach for a general class of statistics when the sample space is finite [19].

While initially the Bootstrap sample size is  $N$ , many works show that a smaller size of Bootstrap sample can give a very good estimation [21]. In [15] Banga et al. propose a Bootstrap model for gray levels image analysis in the case of local segmentation. The use of such resampling procedure enables to reduce considerably the computation times while preserving the estimation quality using the EM algorithm.

### 3. Using Bootstrap resampling for image processing

We can consider an image as a set of  $N$  voxels, where  $N = N_l \times N_c \times N_e$  and  $N_l$ ,  $N_c$  and  $N_e$  define the image resolution. The  $N$  image voxels are indexed with  $i \in S = \{1, 2, \dots, N\}$ , and the data feature vector is denoted by  $y = \{y_1, y_2, \dots, y_N\} \subset \mathfrak{R}^N$ . The key idea behind introducing Bootstrap resampling on mixing parameter estimation problem [14], is to represent the entire image distribution by only  $B$  image samples, where each sample has a small size but should be representative of the entire image.

In Fig. 1 we can see an example of image and its intensity histogram. In Fig. 2 we can note that the mean intensity histogram of the  $B$  samples is superposed on the histogram of the original image shown in Fig. 2(b). To perform a blind segmentation, one can use the EM algorithm. The main idea proposed by Banga et al. in [14] is that only  $B$  small samples of the image are used by the EM algorithm instead of all the voxels of the image. This estimation step of image intensity distribution is therefore considerably faster than the classic EM algorithm. It can be performed using only the Bootstrap samples instead of using the entire image.

### 4. HMRF\_EM framework and Bootstrap resampling

In this section, the image model is first presented; the MAP estimation of the class label in the context of the MRF is then introduced. The complete HMRF\_EM framework for classification as well as the parameter estimation through the EM algorithm is then presented in its original form as proposed in the 'mode field algorithm' in [11] in general and in [12] for the brain tissue application. The incorporation of the Bootstrap schema with the HMRF\_EM framework is shown in the end of this section.

<sup>1</sup>The value of  $B$  is recommended to be at least 50, but depends on the parameter to be estimated [12].

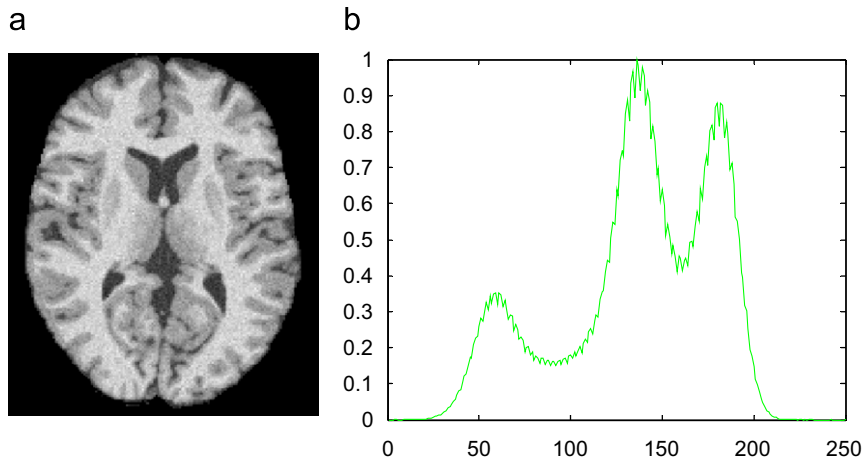


Fig. 1. The original image ‘brain slice’ (a). The intensity histogram of this image (b).

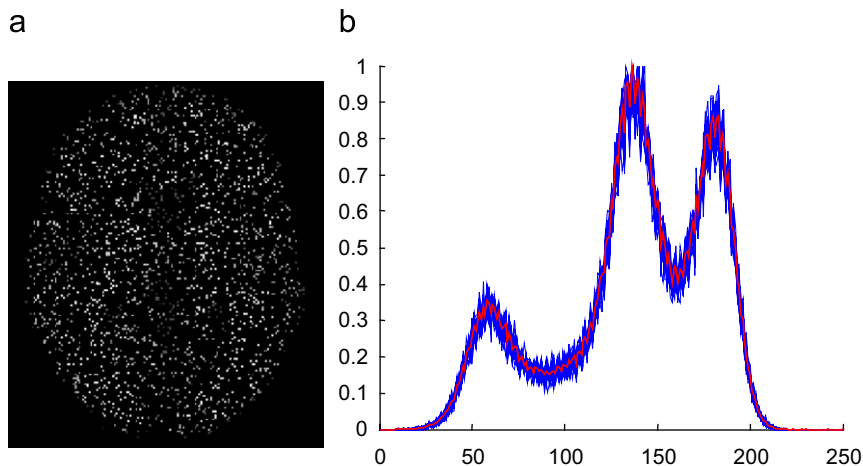


Fig. 2. The Bootstrap sample of a 2D brain slice (a). Intensity histograms of the Bootstrap samples and their mean histogram (b).

4.1. Image model

Let  $L$  and  $D$  be two alphabets:  $L = \{c_1, c_2, \dots, c_k\}$  and  $D = \{1, 2, \dots, d\}$ .

Let  $X$  and  $Y$  be two random fields, respectively with state spaces  $L$ , corresponding to the class labels and  $D$  corresponding to the observations. For  $\forall i \in S$ , we have  $X_i \in L$  and  $Y_i \in D$ . Let  $x$  denote a configuration of  $X$  and  $\chi$  be the set of all possible configurations

$$\chi = \{x = (x_1, x_2, \dots, x_N) | x_i \in L, i \in S\}.$$

Similarly, let  $y$  be a configuration of  $Y$  and  $\zeta$  be the set of all possible configurations so that

$$\zeta = \{y = (y_1, y_2, \dots, y_N) | y_i \in D, i \in S\}.$$

For given  $X_i = \ell$ ,  $Y_i$  follows a conditional probability distribution, assumed from now on as Normal distribution:

$$p(y_i | \ell) = f(y_i; \theta_\ell) \quad \forall \ell \in L,$$

where  $\theta_\ell = \{\mu_\ell, \sigma_\ell\}$  represents the distribution parameters (mean and variance).

In the local approach case, the spatial dependence is ignored and the class field is independently identically distributed. For each label  $\ell \in L$  and for each  $i$  in  $S$ , the probability  $P(X_i = \ell) = \omega_\ell$  is independent of the location of the site  $i$ . This model can be specified fully by the image intensity histogram. However, images with the same intensity distribution may have completely different structural properties.

To overcome this problem, the spatial information can be modeled through the MRF by characterizing mutual influences using conditional MRF distributions.

Since the underlying field  $X$  is non-observable, in the image segmentation context, the appropriate model is the Hidden Markov Random Field (HMRF).

The MRF theory assumes that the sites in  $S$  are related to one another via a neighborhood system, which is defined as  $N = \{N_i, i \in S\}$ , where  $N_i$  is the set of sites neighboring  $i$ ,  $i \notin N_i$  and  $i \in N_j \Leftrightarrow j \in N_i$ . A random field  $X$  is said to be an MRF on  $S$  with respect to a neighborhood system  $N$  if and only if:

$$P(x) > 0 \quad \forall x \in \chi, \\ P(x_i | x_{S-\{i\}}) = P(x_i | x_{N_i}). \quad (1)$$

According to the Hammersley–Clifford theorem [4], an MRF can be characterized by a Gibbs distribution:

$$P(x) = Z^{-1} \text{Exp}(-U(x)), \quad (2)$$

where  $Z$  is the normalizing constant (called partition function) and  $U(x)$  the energy function which is the sum of clique potentials  $V_c(x)$  over all possible cliques  $C^2$ :

$$U(x) = \sum_{c \in C} V_c(x). \quad (3)$$

For 3D images, the considered clique is generally related to the neighborhood system composed of 26-neighbors voxels (the ones around the current voxel). The energy  $U$  could be written as follows:

$$U(x_i = \ell | x_{N_i}) = \sum_{j \in N_i} V_{ij}(x_i, x_j) = \sum_{j \in N_i} \frac{\delta(x_i, x_j)}{d(i,j)}, \quad (4)$$

where  $d(i, j)$  is the distance between the pixels  $i$  and  $j$ , and  $\delta(x_i, x_j)$  is the cost function usually set to  $(0, 1)$ , but could also have other values depending on the application and the image nature.

Our HMRF model is characterized as follows:

- The Hidden (non-observable) random field  $X = \{X_i, i \in S\}$  underlying MRF with a probability distribution given by Eq. (2).
- The observable random field:  $Y = \{Y_i, i \in S\}$ .
- The conditional independence:  $\forall x \in \chi$ , the random variables  $Y_i$  are conditional independent:

$P(y|x) = \prod_{i \in S} P(y_i | x_i)$ . So the joint probability of  $(X, Y)$  is

$$P(x, y) = P(y|x)P(x) = P(x) \prod_{i \in S} P(y_i | x_i). \quad (5)$$

Based on the MRF local characteristic the joint probability of any pair  $(X_i, Y_i)$  given the neighborhood configuration  $X_{N_i}$  of  $X_i$  is

$$P(y_i, x_i | x_{N_i}) = P(y_i | x_i)P(x_i | x_{N_i}). \quad (6)$$

#### 4.2. MAP estimation

Let us denote by  $x^*$ , the true but unknown labeling configuration, and  $\hat{x}$  its estimation. The classification problem is to recover  $x^*$  given the observed image  $y$ .

According to the MAP criterion,  $\hat{x}$  is given by

$$\hat{x} = \text{Arg Max}_{x \in \chi} \{P(y|x)P(x)\}. \quad (7)$$

In the local classification approach,  $\hat{x}$  can easily be calculated. Nevertheless an estimation step is essential to estimate the mixture distribution parameters. This estimation can be classically done by the EM algorithm or by its optimized version the Bootstrapped EM algorithm [15]. In the global classification context, and the HMRF model, this latter formula is equivalent to the following equation:

$$\hat{x} = \text{Arg Min}_{x \in \chi} \{U(y|x) + U(x)\}, \quad (8)$$

where  $U(x)$  is the energy function described in Eq. (3), and  $U(y|x)$  is given by

$$U(y|x) = \sum_{i \in S} \frac{(y_i - \mu_{x_i})^2}{2\sigma_{x_i}^2} + \log(\sigma_{x_i}). \quad (9)$$

This MAP estimation presents a mathematically unfeasible problem. Therefore the optimal solution is usually obtained using the ICM optimization algorithm [4]. Given the data  $y$  and the other labels  $x_{S-\{i\}}^{(k)}$  in iteration  $(k)$ , the ICM algorithm sequentially updates each  $\hat{x}_i^{(k)}$  into  $\hat{x}_i^{(k+1)}$  by minimizing locally the conditional posterior probability  $U(x_i | y, \hat{x}_{N_i}^{(k)})$  with respect to  $x_i$  as proposed in [12] in the case of brain tissues classification and in the description of the ‘mode field algorithm’ in the general case [11]. Note that the updated labels  $\hat{x}_i^{(k)}$  are taken into account in the neighborhood  $\hat{x}_{N_i}^{(k)}$  for the classification of next neighbor sites in the same ICM iteration.

<sup>2</sup>A clique is a subset of sites in  $S$  in which every pair of distinct sites are neighbors in a neighborhood system, except for the single-site cliques.

#### 4.3. Model fitting using HMRF\_EM algorithm

Since both the class label and the parameter set  $\theta = \{\theta_\ell, \ell \in L\}$  are unknown, we can consider that we are in an incomplete data set case, and the problem of parameter estimation can be solved by different techniques, among which the EM algorithm is the most widely used one. Its strategy consists in estimating  $\hat{x}$  given the current estimation of  $\hat{\theta}$  to form the complete data set. The updated (new) value of  $\theta$  can then be estimated by maximizing the expectation of the complete data log likelihood. This iterative algorithm called HMRF\_EM can be resumed as follows:

In an iteration  $t$ :

- estimation of  $\hat{x}$  by ICM
- estimation of  $\hat{\theta}_\ell = (\hat{\mu}_\ell, \hat{\sigma}_\ell)$  by:

$$\begin{aligned}\hat{\mu}_\ell^{(t)} &= \frac{\sum_{i \in S} P^{(t)}(\ell|y_i)y_i}{\sum_{i \in S} P^{(t)}(\ell|y_i)}, \\ (\hat{\sigma}_\ell^{(t)})^2 &= \frac{\sum_{i \in S} P^{(t)}(\ell|y_i)(y_i - \hat{\mu}_\ell^{(t)})^2}{\sum_{i \in S} P^{(t)}(\ell|y_i)};\end{aligned}\quad (10)$$

where

$$P^{(t)}(\ell|y_i) = \frac{f^{(t)}(y_i; \hat{\theta}_\ell)P^{(t)}(\ell|\hat{x}_{N_i})}{P(y_i)}.\quad (11)$$

These expressions are similar to the classical EM formula used in the context of finite Gaussian mixture, but as we can note, the spatial information is encoded in the prior distribution  $P(\ell|\hat{x}_{N_i})$ .

The calculation of the prior distribution  $P(\ell|\hat{x}_{N_i})$ , a particularly consuming task, is expressed in the following equation:

$$P(\ell|\hat{x}_{N_i}) = Z^{-1} \text{Exp}(-U(\ell|\hat{x}_{N_i})).\quad (12)$$

As we can notice, in each iteration, the updating of the means and variances need the scan of the entire image and the updating of the probability  $P^{(t)}(\ell|\hat{x}_{N_i})$  which involves MAP estimation. This estimation task is very time-consuming. That is surely one of the drawbacks of this method, and the reason that many researchers stated that the EM algorithm is difficult to use in the MRF model.

#### 4.4. Bootstrapping the HMRF\_EM

In order to reduce the computing time of the HMRF\_EM, the proposed schema is based on the

conditional independence hypothesis and proposes to use only small Bootstrap samples to update the model parameters. It is important to note that the estimation of the label field in each HMRF\_EM iteration is done using the entire image because the spatial dependency is taken into account through the Markov field. The computation of the probability  $P^{(t)}(\ell|\hat{x}_{N_i})$  will be processed only for the Bootstrap sample used to update the means and variances in Eq. (14). Let us just recall that this probability computation as shown in Eqs. (12) and (4) requires also the scan of the current site neighborhood. Without Bootstrap resampling, in an HMRF\_EM iteration the algorithm scans all image pixels, and for each pixel the scanning of the label neighbors is also necessary to compute the probability  $P^{(t)}(\ell|\hat{x}_{N_i})$  which is a very time-consuming task. On the contrary, with Bootstrap resampling the algorithm need to 'visit' only some pixels, pick up their observation value  $y_i$  and visit also their label neighbors to compute for each of them the conditional probability energy needed to obtain the probability  $P^{(t)}(x_i = \ell|\hat{x}_{N_i})$ .

Let  $S_1^*$  be a representative sample of the image, the estimation step is performed using this sample, and let  $\hat{\theta}_\ell^1$  be the estimated parameter. This estimation task is then repeated  $B$  times with different image samples, and the final estimation  $\hat{\theta}_\ell$  is achieved by the mean of these different estimations ( $b = 1, \dots, B$ ).

$$\hat{\mu}_\ell = \frac{1}{B} \sum_{b=1}^B \hat{\mu}_\ell^{(b)}; \quad \hat{\sigma}_\ell = \frac{1}{B} \sum_{b=1}^B \hat{\sigma}_\ell^{(b)}.\quad (13)$$

The general schema of the bootstrapped version of the HMRF\_EM algorithm, referred to as HMRF\_EM\_B can be resumed in Fig. 3.

In an HMRF\_EM iteration, the mean and variance updating formula of the HMRF\_EM\_B are given by the following formula, where the asterisk indicate the Bootstrap sample elements.

$$\begin{aligned}\hat{\mu}_\ell^{(b)} &= \frac{\sum_{i \in S_b} P^{(t)}(\ell|y_i^*)y_i^*}{\sum_{i \in S_b} P^{(t)}(\ell|y_i^*)}, \\ (\hat{\sigma}_\ell^{(b)})^2 &= \frac{\sum_{i \in S_b} P^{(t)}(\ell|y_i^*)(y_i^* - \hat{\mu}_\ell^{(b)})^2}{\sum_{i \in S_b} P^{(t)}(\ell|y_i^*)};\end{aligned}\quad (14)$$

where

$$P^{(t)}(\ell|y_i^*) = \frac{f^{(t)}(y_i^*; \hat{\theta}_\ell)P^{(t)}(\ell|\hat{x}_{N_i}^*)}{P(y_i^*)}.\quad (15)$$

### 5. The Bootstrap sample size

As we can notice in the updating parameters formula, the Bootstrap sampling concerns on the one hand the observable field. In fact we note that all the summation in the mean and variance update formula are done only for the Bootstrap sample elements specified by  $y^*$ . On the other hand, the Bootstrap resampling concerns also the class field for the computing of  $P(\ell|\hat{x}_{N_i}^*)$  probability. The Bootstrap sample should be representative not only of the intensities level in the observation field, but also of the probability  $P(\ell|\hat{x}_{N_i}^*)$  or more accurately the energy distribution  $U$  in the label field. In fact, in the HMRF\_EM algorithm context the sampling consists in drawing a block of voxels and not simply single ones (Fig. 4).

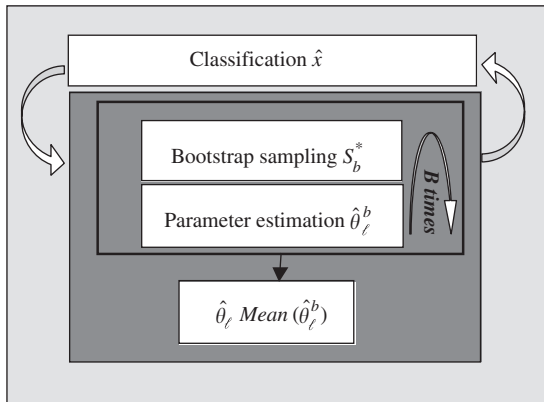


Fig. 3. The general schema of the HMRF\_EM\_B algorithm.

For sample representativity, our work is based on the representativity criteria presented by Banga in [14,15]. These criteria were introduced in the context of local classification for parameters estimation using the Bootstrap version of the EM algorithm. In Banga’s work, the Bootstrap sample has to be representative of the observable field. More particularly, the intensity histogram of the Bootstrap sample should be representative of the entire image intensity histogram.

On the one hand, these criteria were used for the representativity of the image intensity levels in the observation field. On the other hand, these criteria were extended to the multivariate case for the representativity of the energy distribution  $U$  in the label field. Then the sample size will be the one verifying simultaneously the representativity criteria for the observation and the label fields.

In the next paragraph, we will present briefly the two criteria introduced in [14]. They are used for the observation field representativity and their extensions are used in the multivariate case for the label field representation. The extended criteria represent one of this work originally to enable the use of the Bootstrap resampling in the context of the HMRF\_EM algorithm.

#### 5.1. Observation field representativity criteria

Two criteria defined by Banga et al. [15] are used. The first one considers that a sample is representative of the image intensity if and only if each gray

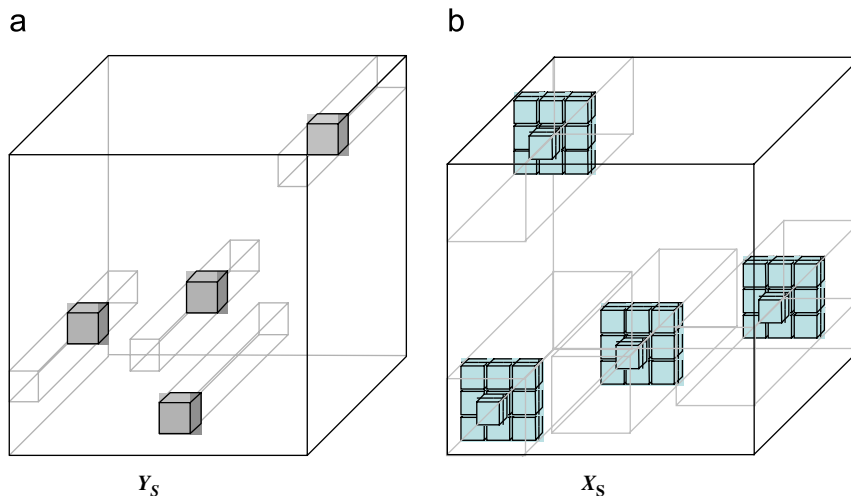


Fig. 4. Example of the sampling in the observations and class fields in 3D image.

level (or intensity) existing in the original image exists at least once in the Bootstrap sample.

The second criterion is more restrictive than the first one. It considers a sample as representative of the image if the proportions of each gray level in the original image are preserved in the Bootstrap sample.

Since the first criterion is already included in the second one, the optimal sample size will be determined using the second criterion, but must anyway verify the first one.

Let us recall that the image is considered as a finite population where each pixel (or voxel in 3D image) takes values in a finite gray level set, and its class takes value in a finite label set. The sampling consists in  $n$  random draws of pixels following the monodimensional marginal empirical law defined on the set  $Y$  of the image observations. This corresponds to a draw with handing-over of observations among  $N$ , which constitutes the initial image. A new set of observations noted  $y^* = \{y_1^*, y_2^*, \dots, y_N^*\}$  is now built; it constitutes the Bootstrap sample of the image.

### 5.1.1. Criterion 1

The sample is representative of the image with  $K$  gray levels if *each gray level  $g$  in the original image appears at least once in the Bootstrapped sample.*

The probability that a particular gray level  $g$  exists in the sample of size  $n$  is  $P_g = 1 - (1 - \pi_g)^n$ , where  $\pi_g$  is its a priori probability. If the condition ( $n\pi_g > 4$ ) is verified,  $P_g$  can be estimated by  $P_g = 1 - e^{-n\pi_g}$ . According to this criterion each gray level in the image should exist in the sample, this is equivalent to the maximization of the joint probability  $P_n = \prod_{i=1}^K (1 - e^{-n\pi_{g_i}})$ . The rare gray levels might then have influence and make tend  $P_n$  to 0. To avoid this, it is more judicious to minimize the derived of the logarithm of the function  $P(x) = \prod_{i=1}^K (1 - e^{-x\pi_{g_i}})$ .

To satisfy this criterion, the sample size called  $n_0$  should therefore verify these two conditions below to obtain a Bootstrap sample representative of the entire image observations, where  $\varepsilon$  is a fixed small value.

$$T(n_0) = \sum_{g=1}^K \frac{\pi_g e^{-n_0 \pi_g}}{1 - e^{-n_0 \pi_g}} < \varepsilon \quad \text{and} \quad n_0 > 4 \cdot K \quad (16)$$

### 5.1.2. Criterion 2

The second criterion considers that the sample is representative if *the proportions ( $\pi_g$ ) of each gray*

*level  $g$  in the image is preserved in the Bootstrap sample.*

The set of the estimated gray level proportions  $\hat{\pi}_g$  follows a multinomial law. According to [22] for a confidence degree  $(1 - \alpha)$ , the confidence interval of this estimator is given by

$$\hat{\pi}_g - \sqrt{\frac{u_{\alpha/2K}^2 \hat{\pi}_g (1 - \hat{\pi}_g)}{n}} < \hat{\pi}_g < \hat{\pi}_g + \sqrt{\frac{u_{\alpha/2K}^2 \hat{\pi}_g (1 - \hat{\pi}_g)}{n}}, \quad (17)$$

where  $u_{\alpha/2K}$  is the fractil of the reduced centered normal law with  $\alpha/2K$  confidence degree.

If this interval is surrounded with a precision  $\pm \Delta\pi$ , the sample size could be easily calculated as follows:

$$n_0 = \frac{(u_{\alpha/2K})^2 \hat{\pi}_g (1 - \hat{\pi}_g)}{(\Delta\pi)^2}. \quad (18)$$

It implies that we could obtain the sample size by fixing a confidence degree  $1 - \alpha$  and a given precision  $\Delta\pi$ . Since the product  $\hat{\pi}_g (1 - \hat{\pi}_g)$  is not a priori information, we take its maximum value, which is obtained for  $\hat{\pi}_g = 1/2$ .

The optimal size of the sample for a  $\Delta\pi$  precision and a  $(1 - \alpha)$  degree of confidence is given by

$$n_0 = \frac{(u_{\alpha/2K})^2}{4(\Delta\pi)^2}. \quad (19)$$

According to these two criteria, to be representative of observation field, the Bootstrap sample size should verify the conditions of Eqs. (16) and (19). This sample size is independent from the image size and depends on the image gray level number  $K$ .

## 5.2. Label field representativity criteria

It is easy to prove that the latter criteria are extendable from univariate classification to the multivariate one. Instead of picking a single voxel label (univariate) a block of labels is picked (multivariate case). For more detail see [23].

Therefore, the two criteria for the energies preservation were defined as follows:

### 5.2.1. Extension of Criterion 1

The sample is representative of the image if *each label block configuration in the entire image label field appears at least once in the Bootstrapped*

sample. Let us  $\lambda$  be this configuration, and  $\pi_\lambda$  the associated proportion.

According to this criterion, the sample size  $n_0$  should verify these two conditions to obtain a Bootstrap sample representative of the entire label field image:

$$T(n_0) = \sum_{\lambda=1}^{\Omega} \frac{\pi_\lambda e^{-n_0 \pi_\lambda}}{1 - e^{-n_0 \pi_\lambda}} < \varepsilon \quad \text{and} \quad n_0 > 4 \cdot \Omega, \quad (20)$$

where  $\Omega$  is the number of possible label configurations in any picked block.

### 5.2.2. Extension of Criterion 2

The second criterion considers that the sample is representative if *the proportions  $\pi_\lambda$  of each label block configuration  $\lambda$  in the image label field is preserved in the Bootstrap sample*. The sample size is the given by

$$n_0 = \frac{(u_{\alpha/2\Omega})^2 \hat{\pi}_\lambda (1 - \hat{\pi}_\lambda)}{(\Delta\pi)^2}, \quad (21)$$

where  $\hat{\pi}_\lambda$  is the estimate of the proportion  $\pi_\lambda$ .

The optimal size of the sample for a  $\Delta\pi$  precision and a  $(1 - \alpha)$  degree of confidence is then given by

$$n_0 = \frac{(u_{\alpha/2\Omega})^2}{4(\Delta\pi)^2}. \quad (22)$$

### 5.2.3. Number of possible label configurations

On the contrary of the observation field representativity where the number of possible picked values  $K$  simply correspond to the number of image gray levels (image dynamic), in this case the representativity of the label field is more complicated. In fact this number depends first on the number of classes in the image segmentation, the block size and the cost function values number (see Eq. (28)).

According to Eqs. (12) and (4) the total number of possibilities of energy computation is not exactly related to the number of different dispositions of labeled pixels, but to the energy ensuing from the summation of Eq. (28). If the case of 2D images is considered, with isotropic pixels, for two values defined cost function (0,1) and an 8-neighbor defined neighborhood system, the total number of possibilities is related to a combination with repetition when the order does not matter. This number is given by

$$K_m^p = C_{m+p-1}^p = \frac{(m+p-1)!}{(m-1)!p!}, \quad (23)$$

where  $m$  is the number of objects to be placed, it corresponds to the different values (or cardinal) of the used cost function for the clique potential computation.  $p$  is the number of possible neighbor sites in the corresponding clique.

For 8-neighbor defined neighborhood system, the total number of possibilities is composed of two combinations, the first is related to the 4-neighbor pixels (where the distance  $d_1$  of each pixel to the central one is the same). The second is related to the four diagonal pixels (where the distances of each pixel to the central one is the same distance  $d_2$  but different from  $d_1$ ).

The number of possibilities for an 8-neighbor defined neighborhood system is then given by

$$NP = K_m^p \times K_m^q = K_2^4 \times K_2^4, \quad (24)$$

where  $q$  is also the number of possible neighbor sites in the corresponding clique ( $p = q = 4$  for an 8-neighbor defined neighborhood system).

The general formulation of Eq. (24) can be expressed as

$$NP = \prod_v K_m^r, \quad (25)$$

where  $v$  is the invariant<sup>3</sup> geometric configuration number,  $r$  is the case number in the clique or geometric configuration.

### 5.2.4. Optimal Bootstrap sample size for label field representativity

According to Criteria 1 and 2, and based on the number of possibilities, the optimal Bootstrap sample size  $n$  is given by

$$\begin{aligned} C1: n > 4\Omega \quad \text{and} \quad \sum_{\lambda=1}^{\Omega} \frac{\pi_\lambda e^{-n_0 \pi_\lambda}}{1 - e^{-n_0 \pi_\lambda}} < \varepsilon, \\ C2: n > \frac{(u_{\alpha/2\Omega})^2}{4(\Delta\pi)^2}. \end{aligned} \quad (26)$$

Let us just remind that by verifying the second condition, the first one is already verified. But since the second criterion depends on two tolerance parameters ( $\Delta\pi, \alpha$ ), it is interesting to check the first criterion to ensure that these parameters are not very large.

<sup>3</sup>Invariance according to the energy calculation.

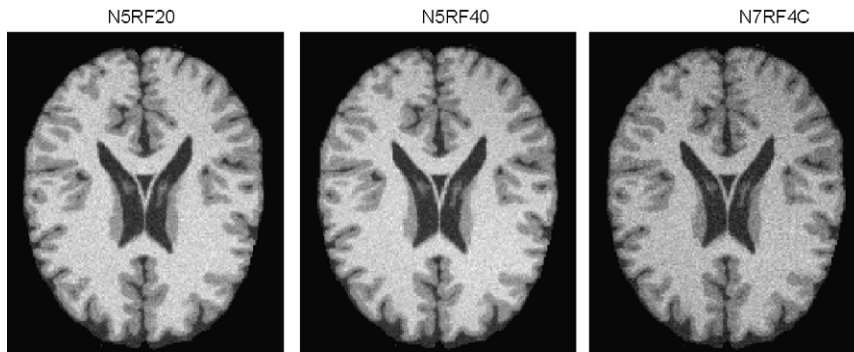


Fig. 5. Slice of the original Brain-web image with different levels of noise and non-homogeneity.

## 6. Experiments and results

### 6.1. Brain tissue classification

#### 6.1.1. Description of the images

To illustrate the performance of the Bootstrap version of the HMRF\_EM algorithm, the tissues classification is performed with and without Bootstrap on some synthetic Brain images. These images, largely used in the context of brain tissues classification come from the McConnell Brain Imaging Center [17]. These ‘Brain-web’ images are based on 27 high-resolution scans of the same individual. A preprocessing task, automatic segmentation and manual correction allowed obtaining segmented brain volume. The segmented volume called ground truth is the reference segmentation. The McConnell Brain Imaging Center provides also several simulated MRI acquisitions of this phantom including RF non-uniformities (bias of 0%, 20% and 40%) and noise levels (0%, 1%, 3%, 5%, 7% and 9%). This makes them particularly suitable for segmentation algorithm assessment.

The segmentation experiments have been applied on different ranges of noise and RF levels on the T1-weighted modality. The volume is  $217 \times 181 \times 217$  voxels with isotropic 1 mm voxel size.

Since we already know the ground truth segmentation, a quantitative comparison between classification methods is possible. According to [16], where the authors tested and compared different segmentation methods for brain segmentation, we assume that the class number is a priori known and fixed to 5: Three classes for the three main tissues (CSF, GM and WM)<sup>4</sup> and two partial volume classes

(CSF-GM and GM-WM). A comparison with ground truth segmentation of tissues classification results based on HMRF\_EM with and without Bootstrap sampling is presented in this section. Fig. 5 presents a slice of original volume with respectively 5% noise 20% radio-frequency non-homogeneity (RF); 5% noise 40% RF and 7% noise 40% RF referred as N5RF20, N5RF40 and N7RF40.

#### 6.1.2. Experiment parameters

Instead of choosing a (0, 1) cost function, it is more appropriate for tissue classification to take a cost function with values that advantage smooth transitions and penalize other configurations, unlikely to occur in the brain tissue (i.e. CSF inside WM [16]). According to the anatomy, the neighboring classes should be (CSF, CSF\_GM, GM, GM\_WM, WM). The partial volume corresponding to CSF\_WM is ignored because of its small proportion 1%. The cost function is defined as follows:

$$\delta(x_i, x_j) = \begin{cases} -2 & \text{if } x_i = x_j, \\ -1 & \text{if } x_i \text{ and } x_j \\ & \text{are neighbors classes,} \\ +1 & \text{else.} \end{cases} \quad (27)$$

It is interesting to note that this energy function can be easily decomposed according to the different geometrical configurations of the neighborhood system. For these 3D images, we assume that the considered clique is related to the neighborhood system composed of 8-neighbors voxels, the front and the back voxels (in the front and back slices). This neighborhood is intentionally not the same in all the directions because the images are initially acquired with 27 scans, and an interpolation is

<sup>4</sup>CSF: cerebroSpinal Fluid, GM: Gray Matter, WM: White Matter.

performed, so the importance or weight of all the directions should not be the same. If this neighborhood is divided on the three different neighborhood configurations, we could obtain three different cliques as presented in Fig. 6.

The energy function can therefore be decomposed (Eq. (28)) according to the three different cliques, where the distances  $d_1$  and  $d_3$  are 1 mm since the image voxels are isotropic and 1 mm size.

$$U(x_i^* = l | x_{N_i}^*) = \sum_{j^* \in Clq1_{i^*}} \frac{\delta(x_i^*, x_j^*)}{d_1(i^*, j^*)} + \sum_{j^* \in Clq2_{i^*}} \frac{\delta(x_i^*, x_j^*)}{d_2(i^*, j^*)} + \sum_{j^* \in Clq3_{i^*}} \frac{\delta(x_i^*, x_j^*)}{d_3(i^*, j^*)}. \quad (28)$$

6.1.3. Bootstrap sample size

To apply the Bootstrap version of the HMRF\_EM algorithm, the sample size of the observation and the label fields are first determined according to the defined representativity criteria. The sample size of the Bootstrap resampling is therefore defined by

$$n_0 = \text{Sup} \left\{ \frac{(u_{\alpha/2K})^2}{4(\Delta\pi)^2}, 4 \cdot K + 1, \frac{(u_{\alpha/2\Omega})^2}{4(\Delta\pi)^2}, 4 \cdot \Omega + 1 \right\},$$

where  $K$  is the number of different gray level values in the image and  $\Omega$  is the number of possible energies ensuing of the different label configurations.

- For the observation field, the sample size depends only on the number of image gray level (image histogram dynamic). The graph of Fig. 7 shows the sample size for the three images of Fig. 5 according to the observed field representativity criteria. From now on the confidence level and the precision are fixed empirically to 5%. Figs. 8 and 9 show the influence of these two parameters on the sample size for a given image (N5RF20,  $K = 250$ ) where we can observe that the variation of  $\Delta\pi$  have much more influence on the sample size than the variation of  $\alpha$ . According to the second criterion, the sample size should be

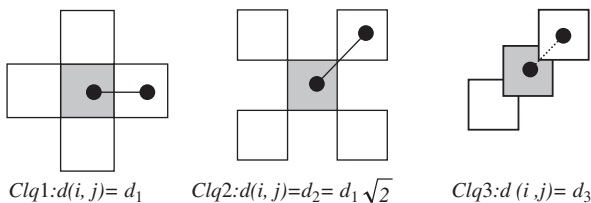


Fig. 6. The neighborhood system for the Brain-web images.

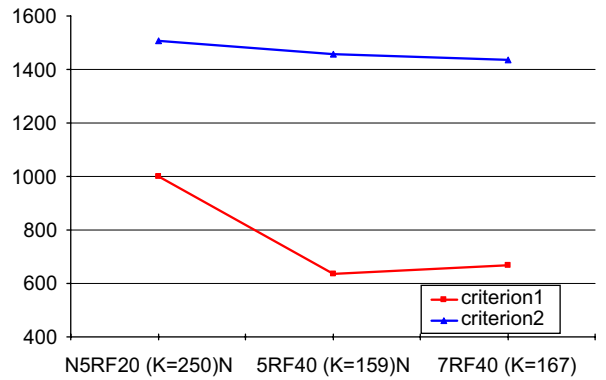


Fig. 7. The Bootstrap sample size according to observation field  $(\alpha, \Delta\pi) = (5, 5)$  (Criteria 1).

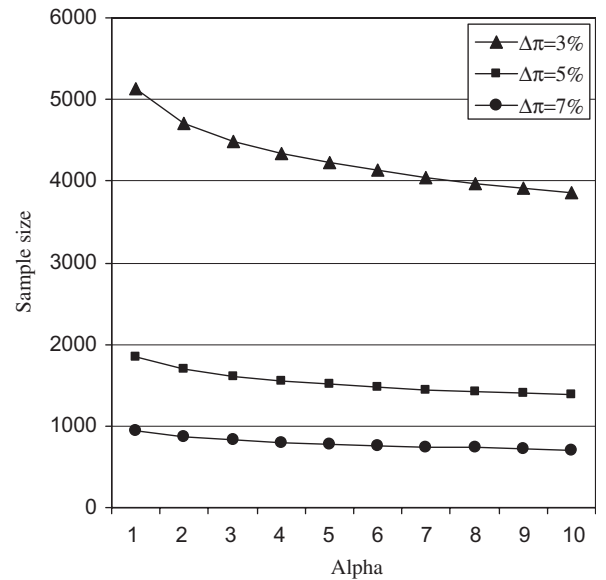


Fig. 8. The influence of  $\alpha$  on the sample size ( $\Delta\pi = 3, 5, 7$ ).

superior than  $(4 \cdot K)$  and should check the condition  $T(n_0) \leq \epsilon$ , which is straightforward to verify with the confidence level and the precision equal to 5%.

- In order to calculate the label field representative sample size the number of energies from the different geometric configurations should first be determined. For the Brain-web images, the voxel size is  $1 \times 1 \times 1$  mm (voxels are isotropic, and the inter-slice distance is 1 mm), the total number of possibilities for neighbors block defined in Fig. 6 is given by Eq. (24), where  $m = 3$ ,  $p = 6$  and  $q = 4$ . On the contrary to the general 3D images case, when the voxels are isotropic to the invariant geometric configuration  $\Omega$  is given by

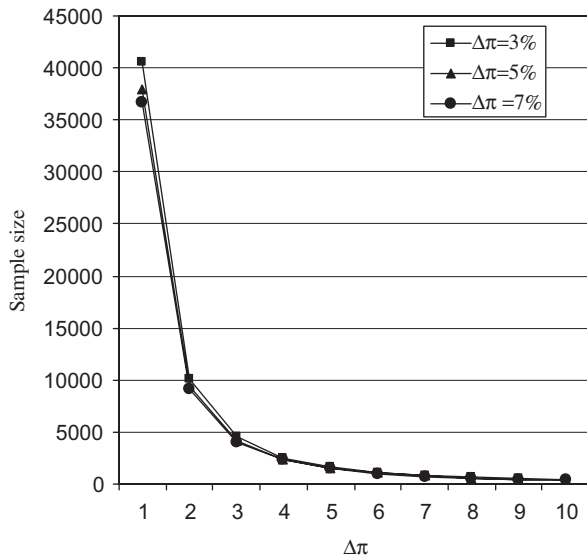


Fig. 9. The influence of Δπ on the sample size (α = 3, 5, 7).

two configurations.

$$\Omega = K_3^6 \times K_3^4 = \frac{8!}{2! \times 6!} \times \frac{6!}{2! \times 4!} = 420. \quad (29)$$

Table 1 gives the sample size according to the defined criteria for the label field representativity. It shows that these sizes are in a range of 0.008% and 0.99% of the total number of voxel in the image (we remove the empty slices in the volume and consider it as 161 × 187 × 161 volume size). The sample size of Bootstrap sample representativity of both gray level and label fields is therefore given by Table 2.

#### 6.1.4. Classification comparison

The validation procedure consists of the comparison of the misclassified rate between the images classified with and without the Bootstrap resampling. To measure the classification accuracy, an Error Classification Rate (ECR) is defined as follows:

$$ECR = \frac{\text{misclassified pixel number}}{\text{image pixel number}}. \quad (30)$$

Let us recall that the ground truth segmentation presented in Fig. 10 is available and makes possible the calculation of the ECR.

The images presented in Fig. 11 show the classification obtained with the HMRF\_EM algorithm with and without Bootstrap resampling. The classified images with the Bootstrap resampling are

Table 1

The sample size of Brain-web images according to the label field representativity (Criterion 2)

α	Δπ									
	1%	2%	3%	4%	5%	6%	7%	8%	9%	10%
1%	48 323	12 081	5369	3020	1933	1342	986	755	597	483
5%	40 194	10 049	4466	2512	1608	1117	820	628	496	402
10%	37 476	9369	4164	2342	1499	1041	765	586	463	375

Table 2

The sample size of Brain-web images according to the observation and label field representativity (Δπ = α = 5%)

Image	Observation field		Label field (Ω = 420)		N <sub>0</sub>	
	K	Criterion 1	Criterion 2	Criterion 1		Criterion 2
N5RF40	159	637	1440	1681	1608	1681
N7RF40	167	669	1447	1681	1608	1681



Fig. 10. The ground truth segmentation.

presented in the first row of the figure. They are visually very similar to those presented in the second row which are classified without the Bootstrap resampling. This result is confirmed in Table 3 by the rate of mis-classified voxels given by the ECR (Eq. (30)).

These classifications are performed with a sample size calculated using the criteria in Section 6.1.3 and corresponding to almost 1700 voxels. The number of replications (B) is empirically fixed to 25, and the number of iterations is equal to 5. With these parameters used for the classification above, the ECR is more or less the same but the computing time is considerably reduced as shown in Table 4.

As expected, the computing time is directly related to the used Bootstrap sample size and the number of replications B. Figs. 12 and 13 show this dependency for the first test image (N5RF20). Furthermore, the sample size has to be representative of the entire image to obtain a good classification accuracy.

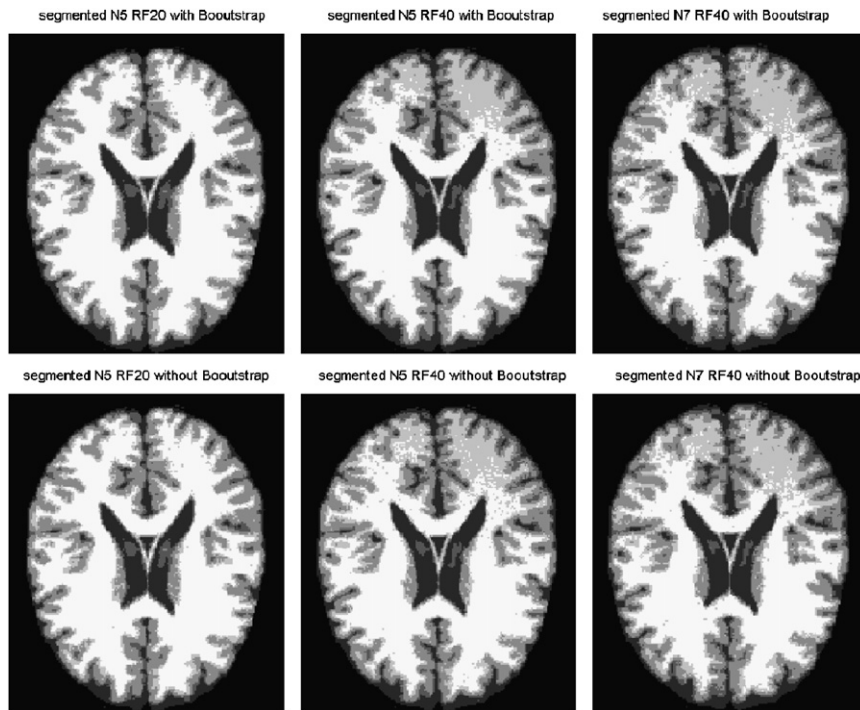


Fig. 11. The segmentation results of Brain-web images with (first row) and without Bootstrap resampling (second row). Column corresponds respectively to images N5RF20, N5RF40 and N7RF40.

Table 3  
The Error Classification Rate (ECR) for the Brain-web images

	HMRF_EM_B	HMRF_EM
RF20_N5	77.19	76.75
RF40_N5	65.56	65.34
RF40_N7	62.11	62.44

Table 4  
The classification computing time for the Brain-web images (normalized)

	HMRF_EM_B	HMRF_EM
RF20_N5	0.63 (159.5 s)	1 (251.6 s)
RF40_N5	0.67 (188.6 s)	1 (280.6 s)
RF40_N7	0.73 (217.9 s)	1 (296.5 s)

6.2. Other experiments

The efficiency of the Bootstrap resampling can also be observed on other type of images. Here are two examples of image segmentation with the EM\_HRMF classification algorithm with and without Bootstrap resampling, the first example is a synthetic 2D image and the second one is a real 2D image.

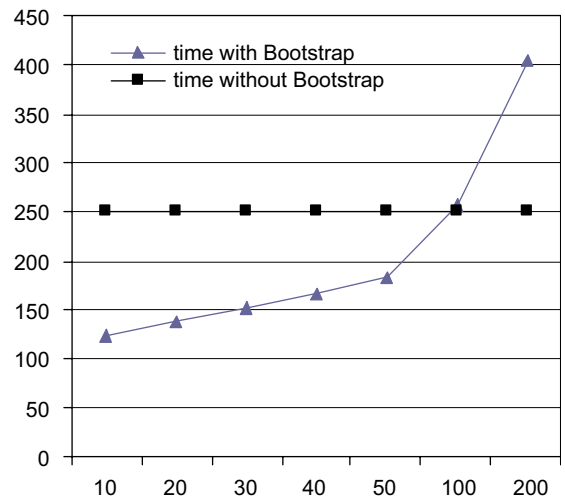


Fig. 12. The computing time for classification (Image N5RF20) for  $N = 1700$  and  $B$  varying from 10 to 200.

Fig. 15 presents the synthetic image composed of five classes used for testing. This image is sampled from an MRF model using the Gibbs sampler, and is considered as the ground truth, the classes proportions are respectively 0.18, 0.18, 0.17, 0.18 and 0.28. A Gaussian noise is added to this image,

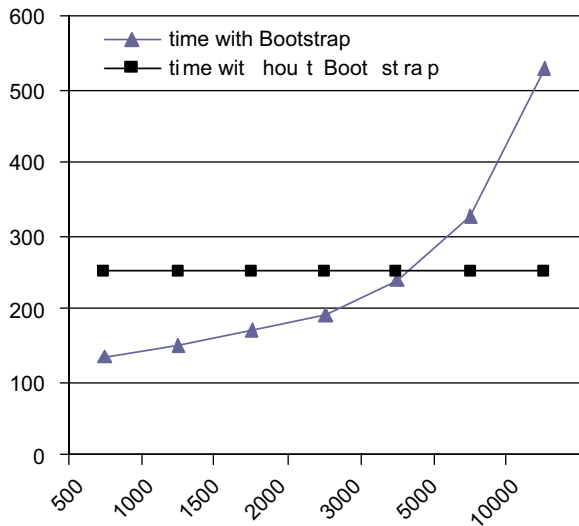


Fig. 13. The computing time for classification (Image N5RF20) for  $B = 25$  and the sample size ( $n$ ) varying from 500 to 10000.

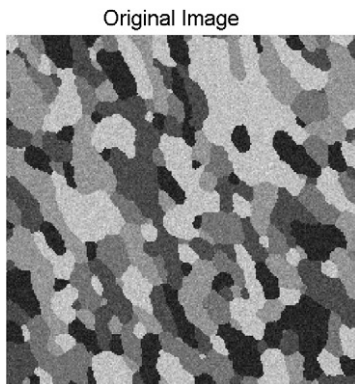


Fig. 14. Original image.

to obtain the test image in Fig. 14. It has a resolution of  $256 \times 256$  with 165 gray levels (see also Fig. 15).

This classification is performed with a sample size calculated using the criteria presented in Section 5 and corresponding to almost 1600 pixels. The number of replication ( $B$ ) is empirically fixed to 25. The cost function is fixed to  $(0, 1)$ , and the neighborhood system is the 8-neighbor one. Fig. 16 shows that the classified image with the Bootstrap resampling is visually very similar to the one classified without the Bootstrap resampling presented in Fig. 17. This result is confirmed by the rate of misclassified pixels given by the ECR (Eq. (30)). In fact, the ECR is more or less the same but the computing time is considerably reduced as shown in Table 5.

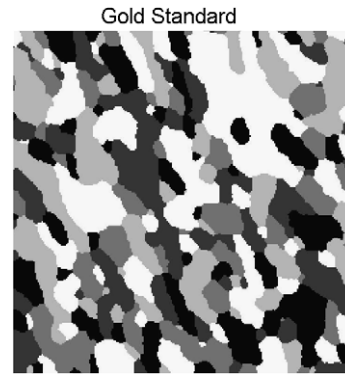


Fig. 15. Ground truth image.

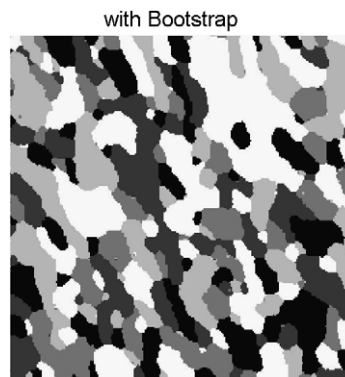


Fig. 16. The segmented image with EM\_HRMF with Bootstrap resampling.

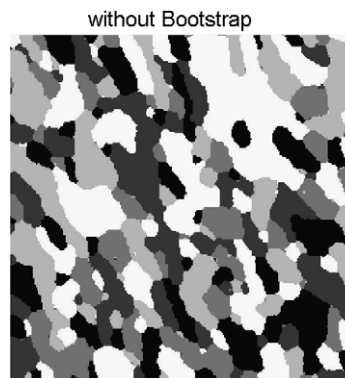


Fig. 17. The segmented image with EM\_HRMF without Bootstrap resampling.

Table 5  
The computing time and the ECR for the synthetic image

	EM_HRMF_B	EM_HRMF
ECR	0.0078	0.009
Computing time (s)	19.49	30.79



Fig. 18. Segmentation result of real image respectively with and without Bootstrap resampling.

For the real image, we apply the classification method on the ‘Lena’ image. Fig. 18 shows a result of EM\_HRMF classification with and without Bootstrap, with a small sample size (1000) and 25 replications. The neighborhood is fixed to the 8-neighbor system, and the cost function is (0,1). We can see visually that the classification is quite the same but the computing time is reduced by 41%.

## 7. Conclusion

In this work, the performance of the HMRF\_EM algorithm is optimized by means of Bootstrap resampling. The way of using the Bootstrap resampling is presented in the context of image classification using an HRMF model. The latter combination is validated for brain tissue classification. By incorporating the HRMF model and the iterative EM algorithm into the HMRF\_EM framework, an accurate and robust segmentation can be achieved. Nevertheless, the classical HMRF\_EM algorithm is time-consuming, due to the entire scan of all image pixels and also their neighbors in each iteration. We show in this paper that the Bootstrap resampling speeds up the classification by 40% with the same accuracy and robustness. This is achieved by using only a small sample to perform the estimation part of the HMRF\_EM algorithm. In addition, we present in this work a study of optimal Bootstrap sample size. The sample size should be as small as possible to have the faster classification, nevertheless, it should be big enough to enable the same classification quality as the classical classification method. Using this sample size study, we presented a comparison of the classical classification and its Bootstrap version using the HMRF\_EM algorithm to show the efficiency of its Bootstrap version. The latter algorithm is validated on a set of three-dimensional synthetic images, particularly suitable for validation thanks to the availability of a gold standard volume.

As shown in Section 6, the computation time is considerably reduced and the classification quality is preserved. In fact, the introduction of the Bootstrap resampling in the EM algorithm is a kind of a stochastic perturbation of the algorithm, which might avoid converging to a local extremum. This is worth thinking about in the next steps of this work with a dependency study of this algorithm. The Stochastic EM (SEM) algorithm is also a stochastic perturbation giving sometimes better estimation than the EM algorithm. Thus it is worth comparing the SEM and the Bootstrapped HMRF\_EM algorithms. Nevertheless, the time reduction is a drawback of the SEM algorithm avoided with the Bootstrapped EM one. This time reduction is particularly important for medical applications because of the large data size and the simultaneous use of different modalities in three-dimensional space. Even though this work did not reach real-time applications it could be considered as a good step toward this main objective. This work is worth continuing by testing other parameters such as new form of energies; parameterized ones where the parameters could be discretized and where our algorithm could be applied to each fixed value. Other work direction could be the proof of the image dynamic estimation quality improvement by the Bootstrap resampling. In fact with the Bootstrap resampling the theoretical independence is better implicated for mixture parameter estimation.

## Acknowledgments

The authors would like to thank Dr. Derrode and Dr. Bach Cuadra for their helpful discussions.

## References

- [1] A. Peng, W. Pieczynski, Adaptive mixture estimation and unsupervised local Bayesian image segmentation, *Graphical Models Image Process.* 57 (1995) 389–399.

- [2] P. Masson, W. Pieczynski, SEM algorithm and unsupervised statistical segmentation of satellite images, *IEEE Trans. Geosci. Remote Sensing* 31 (1993) 618–633.
- [3] N.R. Pal, S.K. Pal, A review on image segmentation techniques, *Pattern Recognition* 26 (1993) 1277–1294.
- [4] J. Besag, On the statistical-analysis of dirty pictures, *J. Roy. Statist. Soc. Ser. B-Methodol.* 48 (1986) 259–302.
- [5] W. Pieczynski, Modèles de Markov en traitements d'images, *Trait. Signal* 20 (3) (2003) 255–277.
- [6] S.Z. Li, *Markov Random Field Modeling in Image Analysis*, Springer-Verlag, 2001.
- [7] B. Chalmond, *Éléments de Modélisation pour L'analyse D'images*, Springer, 2000.
- [8] G.J. McLachlan, T. Krishnan, EM algorithm and extensions, in: *Probability and Statistics*, New York, 1997.
- [9] L. Younes, Parametric inference for imperfectly observed Gibbsian fields, *Probab. Theory Relat. Fields* 82 (1989) 625–645.
- [10] J. Zhang, The mean field theory in EM procedures for Markov random fields, *IEEE Trans. Signal Process.* 40 (10) (1992) 2570–2583.
- [11] G. Celeux, F. Forbes, N. Peyrard, EM procedures using mean field-like approximations for Markov model-based image segmentation, *Pattern Recognition* 36 (1) (2003) 131–144.
- [12] Y. Zhang, M. Brady, S. Smith, Segmentation of brain MR images through a hidden Markov random field model and the expectation-maximization algorithm, *IEEE Trans. Med. Imaging* 20 (2001) 45–57.
- [13] B. Efron, Bootstrap method: another look at the jackknife, *Ann. Statist.* 7 (1979) 1–26.
- [14] C. Banga, *L'approche Bootstrap en Analyse D'images, Application à la Restitution de la Cinétique de la Fuite en Choriorétinopathie Séreuse Centrale*, Thèse de Doctorat, l'université de Rennes I, France, 1995.
- [15] C. Banga, F. Ghorbel, Optimal bootstrap sampling for fast image segmentation: application to retina image, in: *IEEE International Conference on Acoustics, Speech, and Signal Processing*, Minneapolis, USA, 1993.
- [16] M. Bach Cuadra, L. Cammoun, T. Butz, O. Cuisenaire, J.P. Thiran, Comparison and validation of tissue modelization and statistical classification methods in T1-weighted MR brain images, *IEEE Trans. Med. Imaging* 24 (2005) 1548–1565.
- [17] D. Collins, et al., Design and construction of a realistic digital brain phantom, *IEEE Trans. Med. Imaging* 17 (3) (1998) 463–468.
- [18] W.M. Wells, W.E.L. Grimson, R. Kikinis, F.A. Jolesz, Adaptive segmentation of MRI data, *IEEE Trans. Med. Imaging* 15 (4) (1996) 429–442.
- [19] B. Efron, Second thoughts on the bootstrap, *Statist. Sci.* 18 (2003) 135–140.
- [20] M.R. Chernick, *Bootstrap Methods: A Practitioner's Guide*, Wiley Interscience, New York, 1999.
- [21] P.J. Bickel, F. Gotze, W.R. vanZwet, Resampling fewer than  $n$  observations: gains, losses, and remedies for losses, *Statist. Sin.* 7 (1997) 1–31.
- [22] L.A. Goodmann, On simultaneous confidence intervals for multinomial proportions, *Technometrics* 7 (1965) 247–254.
- [23] L. Cammoun, *Classification Bayésienne non supervisée par échantillonnage Bootstrap: cas des tissus cérébraux*, These de doctorat Tunis, Ecole Nationale des Sciences de l'Informatique, Tunisie, 2004.